




# Challenge Journal of CONCRETE RESEARCH LETTERS

## Research Article

# Bio-based cementitious composites reinforced with natural fibers derived from *Cedrus libani* A.Rich. acicular leaf: Extraction, microstructural characterization, and mechanical performance after thermal exposure

Fatih Şamdan <sup>a,\*</sup> , Canan Şamdan <sup>b</sup> , Mehmet Canbaz <sup>a</sup> 

<sup>a</sup> Department of Civil Engineering, Eskişehir Osmangazi University, 26040 Eskişehir, Türkiye

<sup>b</sup> Department of Chemical Engineering, Eskişehir Osmangazi University, 26040 Eskişehir, Türkiye

## ABSTRACT

This study investigates the physical and mechanical performance of bio-based cementitious composites produced with natural fibers obtained from dried, fallen acicular leaf of *Cedrus libani* A.Rich. The fibers underwent a multi-stage pre-treatment prior to composite production, including hot water extraction, alkaline treatment (NaOH), and Ca(OH)<sub>2</sub> mineralization. Changes in surface morphology and chemical composition were confirmed by SEM and EDS analyses, and significant calcium enrichment and increased roughness were observed on the fiber surface after mineralization. Specimens produced with aggregate- and additive-free mixtures were exposed to temperatures of 20, 200, and 400 °C for 3 hours at the end of the curing periods. Unit volume weight, ultrasonic pulse velocity, compressive, flexural, and splitting tensile strengths were determined, and the dynamic modulus of elasticity was calculated. The results showed that limited losses in mechanical properties occurred up to 200 °C, while more significant reductions in strength and stiffness occurred at 400 °C due to microcrack formation and weakening of the fiber-matrix interface. It was determined that mixtures with a high fiber/cement ratio partially limit crack progression and reduce strength loss in certain temperature ranges. The findings reveal the mechanical properties of *Cedrus libani* acicular leaf fibers as reinforcement in cementitious composites after thermal exposure.

## ARTICLE INFO

### Article history:

Received – February 14, 2026  
Revision requested – March 12, 2026  
Revision received – March 15, 2026  
Accepted – March 28, 2026

### Keywords:

Extraction  
Characterization  
Cementitious composites  
Natural fiber  
Mechanical performance  
Thermal exposure



This is an open access article distributed under the CC BY licence.

© 2026 by the Authors.

**Citation:** Şamdan F, Şamdan C, Canbaz M (2026). Bio-based cementitious composites reinforced with natural fibers derived from *Cedrus libani* A.Rich. acicular leaf: Extraction, microstructural characterization, and mechanical performance after thermal exposure. *Challenge Journal of Concrete Research Letters*, 17(2), 162–176.

## 1. Introduction

Composite materials are engineering materials that cannot be obtained from matrix and reinforcement components alone, but superior mechanical and physical properties are provided by using them together. When building materials are evaluated, cementitious composites are widely used, and detailed academic studies are conducted on this subject. In cementitious composite

production, the aim is not only to provide high compressive strength but also to meet various purposes, such as lightness, workability, improved physical properties, resource efficiency, sustainability, and recycling. Fiber-reinforced cementitious composites are preferred to eliminate problems such as brittleness and crack formation and to highlight features such as crack bridging. These composites have been intensively researched in the literature for their contributions, including limiting brittle

\* Corresponding author. E-mail address: fatihsamdan@eskisehir.edu.tr (F. Şamdan)

behavior, controlling crack formation and progression, and increasing ductility. The incorporation of fibers into the cement paste matrix directly affects the composite's mechanical behavior through adhesion, charge-transfer mechanisms, and microcrack-bridging effects at the fiber-matrix interface. These mechanisms suppress sudden fracture behavior, thereby increasing the composite's energy absorption capacity. Thus, fiber reinforcement stands out as an effective material design approach that improves the internal structural continuity of cementitious composites and enables controlled damage development.

Reinforcing cementitious composites with fibers is an effective method that significantly improves the matrix's mechanical performance and damage tolerance. Fiber reinforcement increases tensile and flexural strengths, suppresses brittle fracture behavior, and provides a more ductile deformation process (Bentur and Mindess 2007). It has been experimentally demonstrated that the crack-bridging mechanism formed by fibers in the matrix limits the progression of microcracks and reduces the rate of crack propagation (Li 2003). Similarly, the adhesion developed at the fiber-matrix interface is noted to increase residual bearing capacity and toughness by regulating charge transfer (Banthia and Trottier 1995). The positive effect of fiber supplementation on the energy absorption capacity of composites has been extensively evaluated, leading to marked improvements in impact and fatigue strength (Naaman 2003). It has also been reported that cementitious composites containing fibers exhibit superior properties compared to conventional concretes in reducing shrinkage cracks, controlling crack widths, and improving overall performance (Yousefieh et al. 2017). Taken together, these studies indicate that fiber reinforcement offers an effective material design approach that enables controlled damage development in cementitious composites and improves structural safety.

Fibers are classified as natural, synthetic, and metallic based on their origin, and each type affects the mechanical and physical behavior of cementitious composites through distinct mechanisms. This broad use is also reflected in recent studies on fiber-reinforced construction materials, where fibers are used to improve crack control, flexural response, load transfer, and overall mechanical performance in cementitious and other composite-based systems (Çelik et al. 2024; Ünal and Canbaz 2025; Baş 2025; Alshabrawi and Uysal 2025; Ünal et al. 2025). Natural fibers, in particular, are considered alternative or complementary reinforcing elements in certain applications within fiber-reinforced cementitious composites due to their lower density compared with synthetic and steel fibers, derivation from renewable raw materials, and relatively limited environmental impact. For natural fiber-reinforced lightweight cementitious materials, this contribution is strongly dosage-dependent: suitable contents can improve compressive and flexural performance, whereas excessive fiber incorporation may reduce workability, disturb fiber distribution, and limit hydration because of the high water absorption capacity of plant-based fibers (Uzun 2024). Although natural fibers are classified

by origin as vegetable (lignocellulosic), animal, and mineral, vegetable fibers constitute the main body of the literature on cementitious composites. In this group, jute, flax, hemp, kenaf, sisal, coconut fiber (coir), abaca, cotton, and wood/cellulose-origin fibers stand out (Onuaguluchi and Banthia 2016). Studies show that natural fibers limit crack formation and progression through microcrack bridging in the cementitious matrix, thereby reducing shrinkage-induced cracking, especially in early-age behavior; for example, kenaf and jute fibers have been reported to significantly reduce plastic shrinkage crack width at certain dosages (Lura et al. 2025). In terms of mechanical performance, the use of vegetable fibers such as jute, in appropriate proportions, has been shown to affect fresh and hardened properties and crack control (Islam and Ahmed 2018). Similarly, studies with sisal fibers have reported increases in splitting tensile and flexural strengths and, at suitable dosages, prevention of plastic-shrinkage cracking compared with fiber-free mixtures (Veigas et al. 2022). However, because natural fibers pose risks related to interfacial adhesion and durability in alkaline environments and under wet-drying cycles, the literature emphasizes design strategies such as fiber surface modification, coating, or reducing matrix alkalinity to improve fiber/matrix compatibility. This is also supported by pull-out-based studies on natural fiber-reinforced mineral matrices, which show that fiber surface condition, matrix composition, and interfacial compatibility strongly influence bond resistance and stress transfer at the fiber-matrix interface (Tarhan et al. 2025). For example, post-crack behavior changes due to weakening of the fiber-matrix bond over time have been reported in alkaline-treated natural fiber-reinforced composite systems exposed to natural weathering conditions (Zukowski et al. 2018). Forest-origin natural fibers and plant wastes have also been examined as reinforcement or filler materials, including branches, bark, leaves, cones, sawdust, and chips. The use of lignocellulosic resources associated with forest waste in cementitious composites can reduce unit weight and support crack control through a low-density renewable reinforcement or filler approach, while also influencing processability and fiber-matrix interface strength (Savastano Jr et al. 2003). In studies using bark and woody wastes in fiber or particle form, positive contributions have been reported in terms of thermal insulation, shrinkage behavior, and crack control, although limited decreases in mechanical strength can be observed (Fiore et al. 2015; Merta and Tschegg 2013). Experimental research on cementitious composites with sawdust and wood meal additives has revealed that fiber-matrix adherence improves and performance can be increased when the fiber surface is harmonized with alkaline treatment or mineral additives (Pacheco-Torgal and Jalali 2011; Bilba and Arsène 2008). In studies on leaf-based lignocellulosic supplements, it has been reported that coniferous and broad-leaved plant wastes limit the spread of microcracks and support ductile behavior thanks to their low elastic modulus (Toledo Filho et al. 2005; Silva et al. 2010). In a study in which pine needle leaf fiber (after alkaline pretreatment) was used,

the compressive strength, tensile and splitting tensile strength, and ductility/toughness values of the composite concrete produced increased; it is reported that the effect is explained through fiber–matrix adherence and bridging capacity (Long and Wang 2021).

Exposure of cementitious composites reinforced with natural fibers to elevated temperatures can affect fiber–matrix interaction and the continuity of the internal structure, leading to temperature-dependent changes in mechanical properties. More generally, high-temperature studies on fiber-reinforced concretes indicate that residual mechanical properties and ultrasonic pulse velocity are affected by fiber type, thermal stability, crack development, and fiber–matrix interface changes after heating (Urtekin and Çelik 2025). For this reason, studies have examined the behavior of natural fiber-reinforced cementitious composites under high temperatures. In most of these studies, samples were heated to temperatures in the range of 200–800 °C and evaluated based on compressive, flexural, and tensile strength; mass loss; crack development; and spalling tendency after cooling. The general trend is that as temperature increases, mechanical properties decrease due to dehydration of hydrate products and increased porosity. In addition, because vegetable fibers are organic, degradation at the fiber–matrix interface and thermal degradation of the fibers are reported as critical mechanisms. It has been determined that the high-temperature performance and critical temperature band in plant-based fiber-reinforced concretes are concentrated around 350–450 °C, with damage accelerating above this range. It has also been reported that certain fiber types and geometries may help limit microcracks and reduce the risk of spalling (Al-Dala'ien et al. 2025). In an experimental study on UHPC, exploratory spalling was observed only at 600 °C in steel-fiber mixtures; however, a jute fiber + micro/macro steel fiber hybrid was effective in preventing spalling at 600 °C and provided better results in tensile/flexural strength and toughness parameters (Ridha 2024). In a study of Kenaf fiber-reinforced concretes, experiments conducted between 100 and 800 °C showed a significant deterioration in physical and mechanical properties as temperature increased, highlighting the critical role of thermal damage at the fiber–matrix interface (Aluko et al. 2023). Another study reported that natural fibers can limit spalling by facilitating vapor-pressure discharge as temperature rises, and that the use of sisal+steel hybrid fibers can suppress spalling through a permeability/channel formation mechanism (Ren et al. 2022). Similarly, bamboo fibers regulate internal pressure and crack propagation by creating a "channel" effect through carbonization in the range of 200–800 °C; it has been shown that the hybrid bamboo/steel fiber design can reduce the risk of spalling and maintain residual strength better than steel-fiber-only systems (Zhao et al. 2025). It was also emphasized that natural fibers do not increase strength in all cases; in hemp fiber concretes heated to 400 °C, the strength effect of the fibers may be limited, and a micro-mechanism that reduces crack propagation occurs despite partial fiber decomposition (Grubeša et al. 2018).

It has been reported that the compressive strength of hemp fiber alkali-activated cement foam can improve in the 100–200 °C band depending on the fiber dosage, but the loss of strength becomes evident with thermal degradation of the fiber at 400 °C and 800 °C (Dhasindrakrishna et al. 2023).

When the behavior of cementitious composites reinforced with forest wastes under temperature is examined, the literature reports that strength and mass loss occur in samples directly exposed to high temperatures. In a study on samples reinforced with date palm fiber, it was reported that exposure to 200–300 °C caused a decrease of approximately 6.4–14.8% in compressive strength and 2.1–3.7% in unit volume weight. It has been stated that at these temperature levels, the fibers partially maintain the microcrack-bridging effect, and losses in tensile strength in bending and splitting generally remain in the range of 5.6–9.3%. With the increase in temperature to the range of 400–600 °C, significant thermal degradation was observed in the lignocellulosic structure of the fibers; this situation led to a decrease of 32.4–48.7% in compressive strength and 37.2–58.9% in flexural strength, while unit weight losses were reported to reach 6.5–9.8%. At temperatures above 600 °C, compressive and tensile strength decreased by 61.3–79.6% due to major carbonization or decomposition of the fibers; on the other hand, it has been emphasized that the voids formed by the decomposition of the fibers can relieve vapor pressure, limiting the risk of explosive spalling in some mixtures (Kareem 2025). Another study on date palm fiber shows that as temperature increases, overall mass loss rises and strength decreases due to degradation of the binder hydrate products and increased porosity. In mixtures containing palm leaf-derived fiber, samples were examined after 2 hours of heat exposure; mass loss in the control mixture increased from 0.59% to 4.47% over 200–800 °C, while compressive strength decreased by 46.7% after 800 °C. With higher fiber content, compressive strength decreased by up to 61.8% after 800 °C. These results indicate that fiber addition can increase microstructural gapping and that damage is accelerated by high-temperature water loss and crack network growth; however, strength is retained at moderate temperatures such as 200–400 °C with appropriate mineral additive/binder design (Adamu et al. 2023). Similarly, in another study focusing on mass loss and compressive strength under high temperature, date palm fiber concretes were evaluated over 300–900 °C; it has been reported that the optimum design yields 25.17 MPa strength and 9.84% mass loss at 800 °C, and that approximately 53.5% strength loss occurs as the compressive strength of 54.13 MPa at 24 °C decreases to 25.17 MPa at 800 °C (Adamu et al. 2025). In summary, literature findings show that the mechanical contribution of natural fibers occurs mainly through crack control, and that this contributes positively to mechanical performance. However, fiber-reinforced cementitious composites exposed to different temperatures change in their physical and mechanical properties after temperature, just like normal cementitious composites.

According to the General Directorate of Forestry's 2024 records, cedar (*Cedrus*) is distributed across ap-

proximately 580 thousand hectares in Turkey (General Directorate of Forestry 2025). *Cedrus libani* A.Rich., a species of the genus *Cedrus*, has acicular leaf about 15–35 mm long and is characterized by its rhomboidal cross-sectional geometry and relatively high specific surface area. Unique to the Pinaceae family, it has a distinct wax layer on the leaf surface, and its chemical structure consists mainly of lignocellulosic components, including cellulose, hemicellulose, lignin, and resin. Over time, the natural aging process gradually degrades this wax layer, resulting in increased surface roughness (Güney et al. 2016). Thanks to their high specific surface area and age-related increase in roughness, *Cedrus libani* fibers have the potential to reduce unit weight in the composite, limit microcrack formation, and improve strength and durability by forming an isotropic fiber network in the cemented matrix.

Today, various cement-based composite systems are being developed that utilize forest products and forest-based wastes. These materials are widely used, especially in the construction sector and in the production of different architectural elements. Examples of this approach include wood-precast concrete composites containing wood-based aggregates or fibers, as well as wood-cement-based pressed board products. In such composite systems, mineral aggregate is often not used. Additionally, to better examine the structural characteristics of the material and the fiber-matrix interaction, a fiber-reinforced structure is preferred within the cement matrix. In this study, natural fibers were extracted from *Cedrus libani* A. Rich coniferous leaves, which are considered forest waste. After characterizing the fibers obtained, they were used to produce cement matrix-based composites with different fiber ratios. When reviewing the literature, similar studies have investigated the mechanical behavior of cement-bonded composites made from wood wastes and their performance, particularly under high temperatures (Canbaz et al. 2021; Garcez et al. 2016; Mahzabin et al. 2013). In this study, fiber-reinforced cementitious composites with different cement ratios were prepared using dried and spilled acicular leaf of *Cedrus libani* A.Rich as natural fibers. The specimens were then exposed to temperatures of 20, 200, and 400°C for 3 hours. The fibers were randomly distributed in all directions, creating an isotropic fiber arrangement. Aggregates and additives were not used in the mixture so that the physical and mechanical effects of the fibers, which change with temperature, were fully observed. At the end of the 7- and 28-day curing periods, unit weight, ultrasonic pulse velocity, com-

pressive and flexural strength, and splitting tensile strength were measured for the specimens produced. After exposure to temperatures of 20, 200, and 400°C, the physical and mechanical properties of the specimens were examined.

Numerous studies in the literature explore the physical and mechanical behavior of cementitious wood composites. For instance, Garcez et al. (2016) analyzed how different wood species, particle treatments, and mixing ratios affect the density and mechanical properties of cement-wood composites, revealing that the type of wood and mixing ratio are key factors in composite performance. Similarly, Mahzabin et al. (2013) studied how chemical modification of wood fibers influences the physical and mechanical properties of the cement matrix, demonstrating that chemical treatments to boost fiber-matrix compatibility can markedly improve strength. Additionally, Canbaz et al. (2021) investigated the mechanical behavior of cement-bonded composites containing sawdust exposed to high temperatures, noting that increased temperature can lead to microcrack formation and reduced strength. However, most existing research focuses on wood waste in the form of sawdust or particles, and studies on the use of natural fibers from *Cedrus libani* acicular leaves in cement-based composites, particularly regarding their mechanical behavior under high temperature, are very limited. Therefore, fiber dosage, water absorption behavior, surface condition, and fiber-matrix bond quality should be considered together when evaluating crack-bridging capacity and mechanical performance in natural fiber-reinforced cementitious composites (Uzun 2024; Tarhan et al. 2025). In this context, this study extracts and characterizes natural fibers from *Cedrus libani* acicular leaves and examines their influence on the mechanical performance of cementitious composites, especially under high temperature conditions.

## 2. Materials and Methods


### 2.1. Materials

In this study, Çimsa CEM I 52.5 R cement was used, and its physical and chemical properties are presented in the table. As natural fibers, dried, fallen waste leaf of the *Cedrus libani* A.Rich tree were used. The properties of the fiber are presented in Table 2. City tap water was used as mixing water, and the results of the chemical analysis are presented in Table 3.

**Table 1.** Physical and chemical properties of CEM I 52.5 R cement.

| Physical properties          |         |        | Chemical content (%)           |       |                                |       |
|------------------------------|---------|--------|--------------------------------|-------|--------------------------------|-------|
| Density (g/cm <sup>3</sup> ) | 3.06    |        | CaO                            | 64.70 | SiO <sub>2</sub>               | 21.20 |
| Blaine (m <sup>2</sup> /g)   | 4300    |        | Al <sub>2</sub> O <sub>3</sub> | 4.60  | Fe <sub>2</sub> O <sub>3</sub> | 0.28  |
| Compressive Strength (MPa)   | 7.day   | 28.day | MgO                            | 1.35  | Na <sub>2</sub> O              | 0.38  |
|                              | 50      | 60     | SO <sub>3</sub>                | 3.50  | K <sub>2</sub> O               | 0.20  |
| Setting time (min)           | Initial | Final  | Cl                             | 0.01  | LOI                            | 3.50  |
|                              | 95      | 125    |                                |       |                                |       |

**Table 2.** Physical properties of Cedrus libani A.Rich. and acicular leaf.

|                           |  |                                  |              |   |
|---------------------------|--|----------------------------------|--------------|---|
| Length (mm)               | 15–35  | Unit Weight (g/cm <sup>3</sup> ) | 0.13         |  |
| Width (mm)                | 0.8–2.1  | Density (g/cm <sup>3</sup> )     | 0.48–0.51*   |   |
| Leaf type                 | Acicular   | Modulus of elasticity (GPa)      | 0.67–7.80*   |   |
| Leaf shape                | Needle<br>rhomboidal   | Poisson ratio                    | 0.052–0.522* |   |
|                           |  | Water absorption (%)             | 80.7*        |   |
| Structure and composition | Lignocellulosic fibers<br>(hemicellulose, cellulose, lignin, and wax)* |                                  |              |   |

\* The data was obtained for Cedrus libani A. Rich (Efe 2021; Güney et al. 2016; Güntekin 2022; Şahin and Çam 2022).

**Table 3.** Chemical analysis report for the drinking water treatment plant.

| Chemical analysis results (mg/L) |      |                 |       |            |
|----------------------------------|------|-----------------|-------|------------|
| pH                               | 7.28 | SO <sub>4</sub> | 70    | Al <0.012  |
| Turbidity (NTU)                  | 0.10 | NO <sub>3</sub> | 7.5   | Fe <0.0075 |
| Conductivity (µS/cm)             | 664  | Cl              | 43    | Mn <0.0007 |
| Hardness (Fr°)                   | 32   | NH <sub>4</sub> | <0.05 |            |

## 2.2. Method and tests

### 2.2.1. Fiber pretreatment

The dry, acicular leaf of Cedrus libani A. Rich., collected from the forest ecosystem, were subjected to a comprehensive multistage pretreatment prior to incorporation into cementitious composites. Initially, the materials were manually sorted to eliminate biological and environmental impurities, including soil particles, sand, ash, and fungal residues. First, the collected leaves were sieved to remove foreign substances. Then, to ensure the fiber size falls within a specific range, the material was passed through a sieve with a mesh opening of 2.36–0.60 mm and classified. This process guarantees that the fibers have a more uniform size distribution. The cleaned leaf was thoroughly rinsed with deionized water to remove superficial contaminants and subsequently oven-dried at 60 °C for 24 h. To remove water-soluble extractives, such as tannins and phenolic compounds, that may interfere with cement hydration, hot-water extraction was conducted at 80 °C for 4 h. This procedure was repeated twice using fresh deionized water to ensure effective removal of soluble organic constituents. After extraction, the residues were filtered and dried before undergoing chemical treatment. Alkaline pretreatment was performed by immersing the fibers in a 2.5 wt% NaOH aqueous solution under continuous stirring for 4 h. This step aimed to remove hemicellulosic components and partially increase surface roughness, thereby improving surface reactivity. The treated fibers were rinsed with deionized water until neutral pH was achieved and then oven-dried. For the mineralization stage, the fibers were immersed in a saturated Ca(OH)<sub>2</sub> solution at 30 °C for 12 h using a solid-to-liquid ratio of 2:10 (g mL<sup>-1</sup>). The process was repeated twice with fresh Ca(OH)<sub>2</sub> solution to promote uniform mineral deposition on the fiber sur-

face. Finally, the mineralized fibers were gently rinsed to remove excess surface deposits and dried at 60 °C prior to their incorporation into cementitious composite mixtures.

### 2.2.2. Preparation of specimens

In this study, specimens were produced using natural fibers obtained from the acicular leaf of Cedrus libani A.Rich in different proportions. After the natural fiber-reinforced cementitious composite specimens were exposed to temperatures of 20, 200, and 400°C for 3 hours, their physical and mechanical properties were examined. The cementitious composite mixture is given in Table 4. To observe the effect of the natural fiber, no additives or aggregates other than cement, water, and natural fiber were used. Various cement-based composite systems are being developed, incorporating forest products and waste materials. These materials are mainly used in construction and in making different architectural components. Current applications include wood-precaster concrete composites with wood-based aggregates or fibers, as well as wood-cement-based pressed boards. Typically, mineral aggregate is not used in these composite systems, and a fiber-reinforced structure is preferred within the cement matrix to better understand the material's structural behavior and fiber-matrix interaction. In such systems, the performance is often assessed by comparing mixtures with different fiber contents. Therefore, this study compares mixtures with varying fiber-to-cement ratios and does not include a fiber-free control sample like other studies in the literature (Canbaz et al. 2021; Garcez et al. 2016; Mahzabin et al. 2013). The water/cement ratio and the amount of natural fiber were kept constant, while the cement content was increased.

The specimens were prepared by following the mixing and production procedures specified in the TS EN 196-1 (2016) standard. During production, special attention was given to achieving a homogeneous distribution of fibers within the cement matrix without agglomeration. This aims to ensure that fibers are evenly distributed in various directions within the composite structure, resulting in a more uniform and isotropic behavior of the material. Additionally, after placing the mixture into the formwork, pressure was applied, similar to the process used for manufacturing wood-cement-based pressed boards, to ensure the mixture was more uniformly and neatly placed within the formwork.

*Cedrus libani* A.Rich. The acicular-leaf mixture was symbolized by CL, and specimen types were identified by adding the amount of cement used to the codes. Standard

specimens of 4x4x16 cm were produced and cured at  $20 \pm 2$  °C for 28 days. Photographs of CL-type specimens are shown in Fig 1.

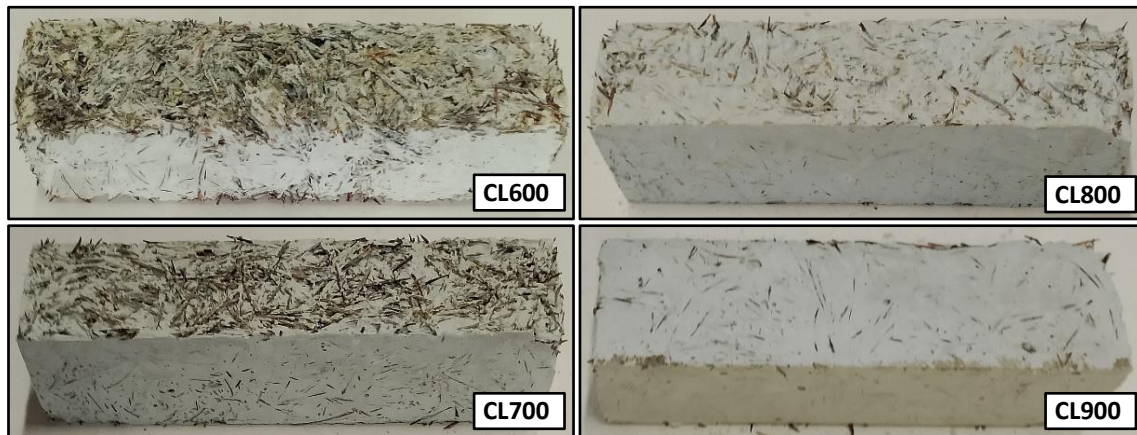


**Fig. 1.** Photographs of CL600–900 specimens after production.

**Table 4.** Proportions of materials as per the mixture.

| Code  | Water / Cement<br>(by wt.) | Fiber<br>(g) | Cement<br>(g) | Fiber / Cement<br>(by wt.) | Fiber / Cement<br>(by vol.) |
|-------|----------------------------|--------------|---------------|----------------------------|-----------------------------|
| CL600 |                            |              | 600           | 0.22                       | 0.32                        |
| CL700 | 0.40                       | 130          | 700           | 0.19                       | 0.28                        |
| CL800 |                            |              | 800           | 0.16                       | 0.24                        |
| CL900 |                            |              | 900           | 0.14                       | 0.22                        |

### 2.2.3. Thermal exposure of specimens

After curing, the specimens were kept in the laboratory oven for 1 hour to ensure they were dry. Then, thermal exposure was applied to the specimens using a Nevola Reis 110/10 thermocouple-controlled furnace. During thermal exposure, the temperature was gradually increased to an average rate of 80–100 °C/min. Because the furnace system has a control mechanism that minimizes temperature fluctuations, the target temperatures are reached more steadily. After reaching the target temperatures of 200 and 400 °C, the specimens were maintained at these levels for 3 hours. Once the thermal exposure was complete, the specimens were removed from the furnace and allowed to cool naturally at room temperature in a laboratory environment.

Temperature levels of 20, 200, and 400 °C were applied in the experimental program. These levels were chosen because 20 °C represents the reference condition at room temperature, 200 °C indicates a moderate thermal effect in cementitious materials where free water loss and initial microstructural changes occur, and 400 °C marks a critical temperature range nearing the thermal degradation and ignition points reported in the literature for lignocellulosic fibers.

The main goal of this study is to analyze how natural fiber reinforced cement-based composites behave under high temperatures and to identify the damage mechanisms, especially at the fiber-matrix interface. Natural fi-

bers from plants have a lignocellulosic structure mainly made up of hemicellulose, cellulose, and lignin (Şahin and Çam 2022). These components degrade at different temperatures as the temperature rises, leading to significant changes in the fiber's structural integrity. The literature reports that the thermal degradation and ignition temperatures of lignocellulosic biomass components are about 370 °C for hemicellulose, 410 °C for cellulose, and 405 °C for lignin (Yang et al. 2007; Cao et al. 2019). This indicates that the fiber structure can quickly degrade at temperatures of 400 °C and above, greatly increasing the risk of burning or ignition. The study selected a temperature range where both fiber-matrix interactions and changes in mechanical performance could be observed, while still maintaining specimen integrity. Specifically, experiments were conducted at 20, 200, and 400 °C, with the upper limit of 400 °C chosen to account for the critical temperature zone where lignocellulosic fibers begin to ignite and degrade rapidly. This approach allowed for a safe and controlled evaluation of the thermal damage mechanisms and performance changes of natural fiber-reinforced cement-based composites at high temperatures.

### 2.2.4. Mechanical tests of specimens

Prismatic specimens, measuring 40×40×160 mm, were subjected to a three-point flexural test in accordance with the TS EN 196-1 (2016) standard after exposure to temperatures of 20, 200, and 400°C. During the experiments, loading was carried out using the clearance and loading speed specified in the standard. Samples produced at different fiber/cement ratios were examined for their mechanical behavior after exposure to different temperatures.

Cubic samples measuring 40×40×40 mm, produced with various fiber/cement ratios, were exposed to temperatures of 20, 200, and 400°C, and then a compression test was performed in accordance with TS EN 196-1 (2016). The experiments were performed on a universal test press, and the samples were loaded until they failed

under the established standard conditions. The mechanical properties of the samples produced at different fiber/cement ratios and exposed to various temperatures were evaluated.

To determine the splitting tensile strength of the specimens, loads were applied perpendicularly to the cross-sections, and the splitting tensile strengths generated along the sample cross-section were measured.

In the experimental program, specimens were produced considering three different temperature levels, four types of specimens, and three repetitions for each type. In this process, a total of 36 specimens were tested for each mechanical test. The average results of the experiments for each variable were calculated, and the standard deviation (SD) and coefficient of variation (CV) values are shown in Table 5.

**Table 5.** Statistical analysis of data.

| Compressive strength (MPa)       |       |       |      |        | Flexural strength (MPa)           |       |       |      |        |
|----------------------------------|-------|-------|------|--------|-----------------------------------|-------|-------|------|--------|
| Temperature (°C)                 | Code  | Mean  | SD   | CV (%) | Temperature (°C)                  | Code  | Mean  | SD   | CV (%) |
| 20                               | CL600 | 8.27  | 0.52 | 6.2    | 20                                | CL600 | 1.36  | 0.07 | 5.1    |
|                                  | CL700 | 9.40  | 0.49 | 5.2    |                                   | CL700 | 2.25  | 0.18 | 7.8    |
|                                  | CL800 | 10.49 | 0.80 | 7.6    |                                   | CL800 | 3.09  | 0.21 | 6.8    |
|                                  | CL900 | 11.10 | 0.75 | 6.7    |                                   | CL900 | 3.45  | 0.26 | 7.5    |
| 200                              | CL600 | 7.84  | 0.58 | 7.4    | 200                               | CL600 | 1.23  | 0.07 | 5.3    |
|                                  | CL700 | 9.02  | 0.69 | 7.7    |                                   | CL700 | 1.92  | 0.12 | 6.1    |
|                                  | CL800 | 9.69  | 0.61 | 6.3    |                                   | CL800 | 2.70  | 0.17 | 6.2    |
|                                  | CL900 | 10.13 | 0.60 | 5.9    |                                   | CL900 | 3.02  | 0.23 | 7.7    |
| 400                              | CL600 | 7.56  | 0.36 | 4.8    | 400                               | CL600 | 1.18  | 0.08 | 6.6    |
|                                  | CL700 | 8.35  | 0.43 | 5.2    |                                   | CL700 | 1.74  | 0.12 | 7.0    |
|                                  | CL800 | 8.78  | 0.65 | 7.5    |                                   | CL800 | 2.33  | 0.16 | 6.9    |
|                                  | CL900 | 9.09  | 0.42 | 4.6    |                                   | CL900 | 2.52  | 0.16 | 6.5    |
| Splitting tensile strength (MPa) |       |       |      |        | Unit weight (kg/dm <sup>3</sup> ) |       |       |      |        |
| Temperature (°C)                 | Code  | Mean  | SD   | CV (%) | Temperature (°C)                  | Code  | Mean  | SD   | CV (%) |
| 20                               | CL600 | 1.46  | 0.09 | 6.3    | 20                                | CL600 | 1.420 | 0.08 | 5.6    |
|                                  | CL700 | 1.55  | 0.07 | 4.4    |                                   | CL700 | 1.473 | 0.09 | 6.0    |
|                                  | CL800 | 2.04  | 0.09 | 4.7    |                                   | CL800 | 1.570 | 0.09 | 6.0    |
|                                  | CL900 | 2.28  | 0.16 | 7.2    |                                   | CL900 | 1.596 | 0.07 | 4.4    |
| 200                              | CL600 | 1.38  | 0.07 | 5.3    | 200                               | CL600 | 1.280 | 0.07 | 5.8    |
|                                  | CL700 | 1.50  | 0.08 | 5.3    |                                   | CL700 | 1.364 | 0.09 | 6.4    |
|                                  | CL800 | 1.94  | 0.10 | 5.0    |                                   | CL800 | 1.500 | 0.06 | 4.1    |
|                                  | CL900 | 2.13  | 0.16 | 7.5    |                                   | CL900 | 1.547 | 0.07 | 4.5    |
| 400                              | CL600 | 1.34  | 0.07 | 5.0    | 400                               | CL600 | 1.218 | 0.08 | 6.3    |
|                                  | CL700 | 1.38  | 0.07 | 5.0    |                                   | CL700 | 1.282 | 0.09 | 7.1    |
|                                  | CL800 | 1.69  | 0.11 | 6.4    |                                   | CL800 | 1.429 | 0.07 | 5.0    |
|                                  | CL900 | 1.84  | 0.08 | 4.5    |                                   | CL900 | 1.456 | 0.09 | 5.9    |
| UPV (km/h)                       |       |       |      |        | $E_{dynamic}$ (Gpa)               |       |       |      |        |
| Temperature (°C)                 | Code  | Mean  | SD   | CV (%) | Temperature (°C)                  | Code  | Mean  | SD   | CV (%) |
| 20                               | CL600 | 2.38  | 0.15 | 6.3    | 20                                | CL600 | 8.16  | 0.57 | 7.0    |
|                                  | CL700 | 2.45  | 0.15 | 6.2    |                                   | CL700 | 9.02  | 0.58 | 6.4    |
|                                  | CL800 | 2.62  | 0.14 | 5.4    |                                   | CL800 | 10.98 | 0.53 | 4.8    |
|                                  | CL900 | 2.69  | 0.21 | 7.9    |                                   | CL900 | 11.76 | 1.34 | 11.4   |
| 200                              | CL600 | 2.23  | 0.15 | 6.7    | 200                               | CL600 | 6.49  | 0.50 | 7.7    |
|                                  | CL700 | 2.28  | 0.13 | 5.7    |                                   | CL700 | 7.24  | 0.36 | 5.0    |
|                                  | CL800 | 2.52  | 0.14 | 5.5    |                                   | CL800 | 9.74  | 0.68 | 7.0    |
|                                  | CL900 | 2.63  | 0.11 | 4.2    |                                   | CL900 | 10.90 | 0.43 | 3.9    |
| 400                              | CL600 | 2.08  | 0.10 | 4.8    | 400                               | CL600 | 5.38  | 0.17 | 3.2    |
|                                  | CL700 | 2.16  | 0.14 | 6.6    |                                   | CL700 | 6.09  | 0.37 | 6.1    |
|                                  | CL800 | 2.42  | 0.17 | 7.0    |                                   | CL800 | 8.53  | 0.77 | 9.0    |
|                                  | CL900 | 2.50  | 0.15 | 6.0    |                                   | CL900 | 9.24  | 0.57 | 6.2    |

### 3. Results and Discussion

#### 3.1. Microstructural and chemical characterization

As shown in Fig. 2a, the untreated fibers display a relatively smooth and dense surface structure common to lignocellulosic materials that maintain their waxy and hemicellulosic layers. These traits typically inhibit mechanical interlocking within cementitious matrices due to a reduction in surface roughness. Comparable morphological characteristics in unprocessed plant fibers were also documented, observed that fewer surface irregularities were linked to a decrease in interfacial bonding potential (Melichar et al. 2024).

In contrast, Fig. 2b shows that treatment with  $\text{Ca}(\text{OH})_2$  significantly alters the fiber surface. After undergoing alkaline treatment and subsequent mineralization, there is a notable increase in surface roughness along with the formation of localized mineral aggregates. Alkaline conditions can prompt structural rearrangements, which in turn boost surface reactivity. This mechanism aligns with the morphological changes observed in the present study, in which alkali-mediated surface activation increases the potential for fiber-matrix interactions. (Hu et al. 2024).

The EDS spectra show a distinct compositional shift following the mineralization process. As illustrated in Fig. 2c, the untreated fibers primarily exhibit peaks from

carbon and oxygen, indicating their lignocellulosic composition, with carbon as the predominant element and oxygen as the secondary one. The absence of measurable calcium indicates that the untreated surface is entirely organic, consistent with the lignin–cellulose–hemicellulose structures observed in native biomass fibers (Das et al. 2024). After  $\text{Ca}(\text{OH})_2$  treatment (Fig. 2c), a pronounced calcium peak emerges, with Ca reaching approximately 50–53 wt%, while carbon decreases to around 19–20 wt% and oxygen increases to roughly 27–28 wt%. This marked shift from a carbon-dominated to a calcium-rich surface composition confirms successful mineral deposition. Similar calcium enrichment accompanied by relative carbon reduction has been documented following Ca-based surface mineralization of natural fibers, where inorganic precipitation partially masks the organic substrate and alters the surface chemistry (Li et al. 2025; Zhang et al. 2025).

Elemental mapping (Fig. 2d-e) further confirms that calcium is distributed across the treated fiber surface rather than uniformly embedded within the bulk structure. The formation of calcium-rich domains indicates surface precipitation and partial mineral coverage. This local mineralization has been associated with increased interfacial stiffness and improved load transfer in cemented composites in some studies (Feng et al. 2025; Melichar et al. 2024).

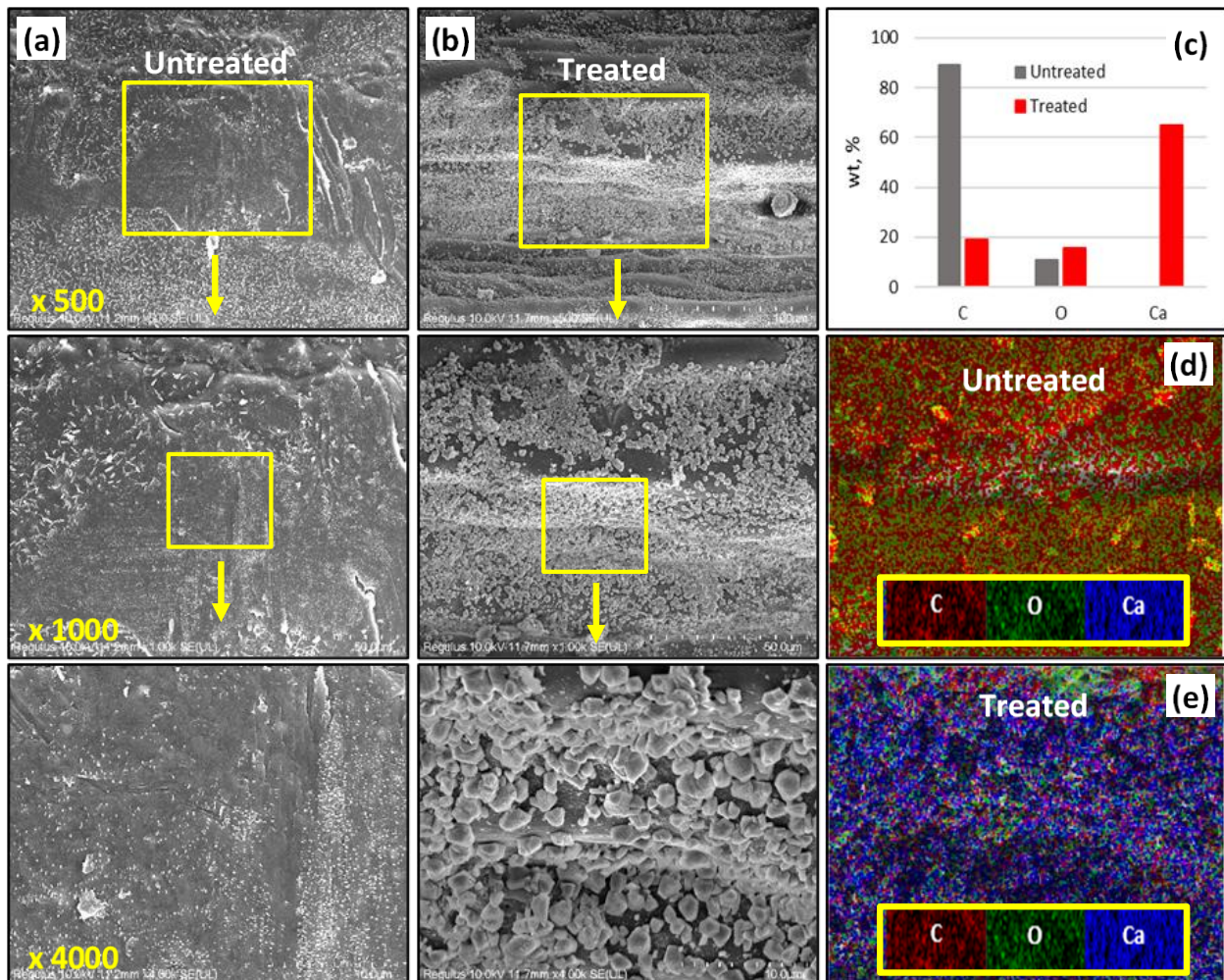


Fig. 2. Untreated (a) and treated (b) fiber SEM images; (c) EDS analysis; (d, e) Elemental mapping.

Changes in fiber morphology after surface treatments significantly influence the microstructural behavior of the composite material. Increased roughness on the fiber surface following alkaline and calcium hydroxide treatments, along with mineral phase deposits, promote mechanical interlocking at the fiber-matrix interface. This enhances the bond between cement hydration products and the fiber surface, leading to more efficient load transfer. Performance under high temperatures is affected not only by the reduction in mechanical properties but also by microstructural and chemical transformations within the composite. Natural fibers with lignocellulosic structures primarily contain hemicellulose, cellulose, and lignin, which degrade thermally at different temperature ranges. Partial degradation of the fiber structure, especially at elevated temperatures, can cause loss of adhesion, formation of microgaps, and development of microcracks at the fiber-matrix interface. In the cement-based matrix, processes such as hydrate phase dehydration, bond weakening, and internal stress buildup also occur as temperature rises. When considering these microstructural and thermochemical changes together, it becomes clear that the variation in mechanical performance of composite materials at high temperatures is closely linked to thermal degradation of the fiber structure and weakening of interfacial interactions.

On the other hand, the natural fibers in the composite structure play a crucial mechanical role, especially during crack propagation. The fibers act as a bridge between crack surfaces by restricting the progression of microcracks in the matrix and enabling charge transfer to continue through the fibers. The crack-bridging effect delays the sudden fracture of composite materials because the fibers show more ductile behavior than the matrix. Mechanical clamping of the fibers to the matrix and improved bonding at the interface reduce crack growth and enhance the composite's energy absorption capacity. This is also supported by fracture behavior observed, especially in flexural and splitting tensile tests. During these experiments, it was observed that the specimens did not break suddenly and destructively; instead, they formed a bridge between the cracked surfaces with the fibers, preventing complete separation. The fibers continued to carry loads between the cracked surfaces, causing the specimens to retain some integrity and display

more ductile behavior even after fracture. This indicates that the fiber-matrix interaction in natural fiber-reinforced cement-based composites significantly contributes not only to initial mechanical strength but also to the fracture process and damage development.

### 3.2. Compressive strength

First of all, the cement-based composites developed in this study are designed for applications similar to wood-cement composites and wood-based cement binder products in terms of their intended use. These materials are widely used in producing different architectural elements, especially in the construction industry, with examples including wood-precaster concrete composites containing wood-based aggregates or fibers and wood-cement-based pressed board products. Since these materials are not typically used as load-bearing structural elements, high compressive strength is not an expected characteristic of such composite systems. The compressive stresses measured in these products are generally low (Canbaz et al. 2021; Garcez et al. 2016; Mahzabin et al. 2013). The main reason for the low compressive stress is that the woody content in the mixture bonds weaker than cement, which increases the void ratio (Canbaz et al. 2021).

The compressive strength results presented in Fig. 3 show that cementitious composites reinforced with natural fibers from acicular *Cedrus libani* A.Rich exhibit a significant but gradual loss of strength with increasing temperature. For all mixtures, the decrease in compressive strength after 200 °C was limited; in specimens, it ranged from about 5.25% to 8.76%. Compressive strength is largely preserved due to the removal of free water and limited microstructural changes up to 200 °C. At 400 °C, total strength losses ranged from 8.58% to 18.08% compared with specimens at 20 °C. Compressive strength losses are mainly related to microcracks developing in the cement paste with increasing temperature, weakening of adhesion at the fiber-matrix interface, and gradual degradation of lignocellulosic coniferous fibers in the range of 200–400 °C. The higher strength loss at 400 °C (16.33–18.08%), especially in the CL800 and CL900 series with high cement content, indicates that a more rigid and dense matrix structure is more sensitive to crack development under thermal stresses.

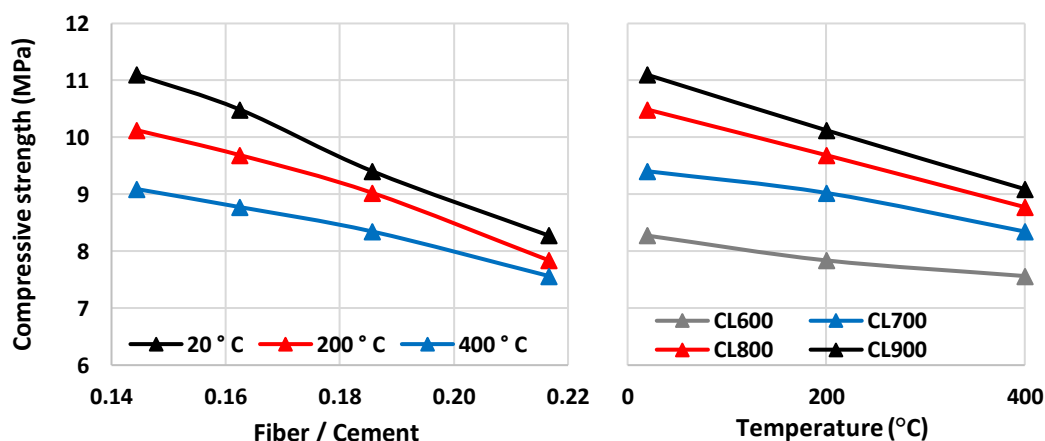


Fig. 3. Compressive strength of specimens based on changes in fiber/cement ratio and temperature after thermal exposure.

On the other hand, in CL600 and CL700 specimens, microcracks are partially limited thanks to the higher fiber/cement ratio, and the strength loss is more limited at 400 °C. These findings show that Cedrus libani needle-leaf fibers can contribute to the maintenance of compressive strength by delaying crack propagation at certain fiber/cement ratios under high temperature.

### 3.3. Flexural strength

The flexural strength results presented in Fig. 4 reveal a significant and systematic decrease in strength with increasing temperature in cementitious composites reinforced with Cedrus libani acicular leaf fiber. When flexural strengths measured at 20 °C are compared with those exposed to 200 °C, a loss of approximately 9.8–14.8% is observed. For samples exposed to 400 °C, the flexural strength loss ranges from 13.4% to 27.1%. This indicates that, with the fiber content held constant across temperature levels, increasing the cement dosage signif-

icantly increases flexural strength. Flexural strength is more sensitive to temperature increases than compressive strength, and this effect is particularly evident in the 200–400 °C range. Because flexural behavior is governed by tensile stresses, microcracks in the cement paste, along with weakening of adhesion at the fiber-matrix interface as temperature rises, lead to proportionally greater losses in flexural strength. The greater strength losses observed at 400 °C in CL800 and CL900 specimens with high cement content (24.6–27.1%) suggest that the denser, more rigid matrix structure is more susceptible to crack formation under thermal stresses. In contrast, the higher fiber/cement ratio in the CL600 and CL700 samples appears to partially limit microcrack development, and therefore the relative losses in flexural strength remain at lower levels. In this context, Cedrus libani acicular leaf fibers play a supporting role in flexural behavior at low and medium temperatures, but this contribution becomes limited as the fiber-matrix interaction weakens when the temperature reaches 400 °C.

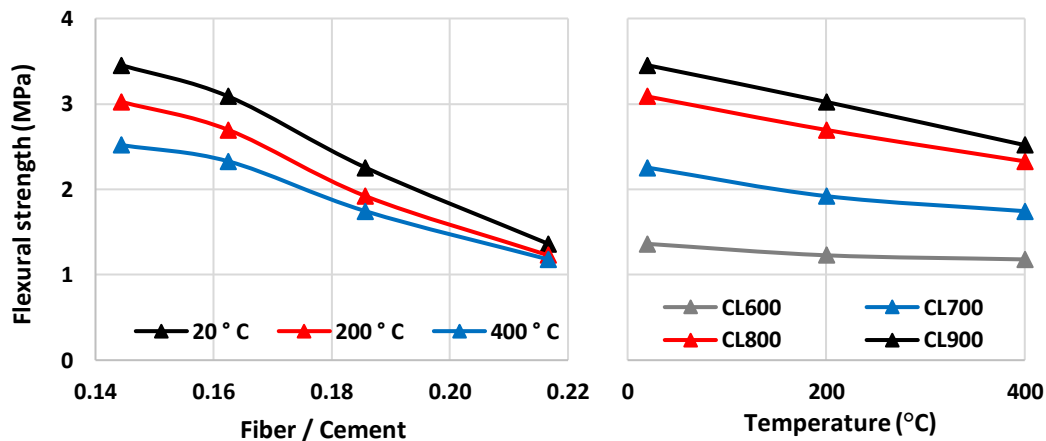


Fig. 4. Flexural strength of the specimens influenced by changes in fiber/cement ratio and temperature after thermal exposure.

### 3.4. Splitting tensile strength tests

The splitting tensile strength results presented in Fig. 5 show that the tensile behavior of Cedrus libani acicular leaf fiber-reinforced cementitious composites weakens systematically with increasing temperature. With the temperature increase to 200 °C, the strengths decreased by approximately 3.1–6.5% compared to the 20 °C reference, and after the application of 400 °C, the strength losses reached 8.6–19.1%. This trend in splitting tensile strength can be associated with the weakening of the fiber-matrix interaction, which is sensitive to tensile stresses, as the temperature increases. The occurrence of higher proportional strength losses (additional decrease in the range of 12.5–13.4%) in the CL800 and CL900 specimens, especially in the range of 200–400 °C, suggests that the more rigid and dense matrix structure exhibits a more sensitive response to microcrack formation under thermal stresses. On the other hand, it is seen that microcracks are partially limited in CL600 and CL700 mixtures thanks to the higher fiber/cement ratio,

and the additional strength loss remains at lower levels after 400 °C. In this context, it was found that Cedrus libani acicular leaf fibers contribute to splitting tensile strength by delaying the progression of tensile cracks at low and medium temperatures; however, when the temperature reaches 400 °C, this contribution decreases significantly with increasing damage to the fiber-matrix interface.

### 3.5. Unit weight

The unit weight results after applying the temperature shown in Fig. 6 indicate that a significant density loss occurs as temperature increases in cementitious composites reinforced with Cedrus libani acicular leaf fiber. Unit weight values measured at 20 °C were 1,420–1,596 kg/dm<sup>3</sup>. With the rise in temperature to 200 °C, unit weights decreased to 1,280–1,547 kg/dm<sup>3</sup>. This corresponds to unit weight losses of approximately 9.9% for CL600, 7.4% for CL700, 4.4% for CL800, and 3.1% for CL900, compared with the 20 °C reference.

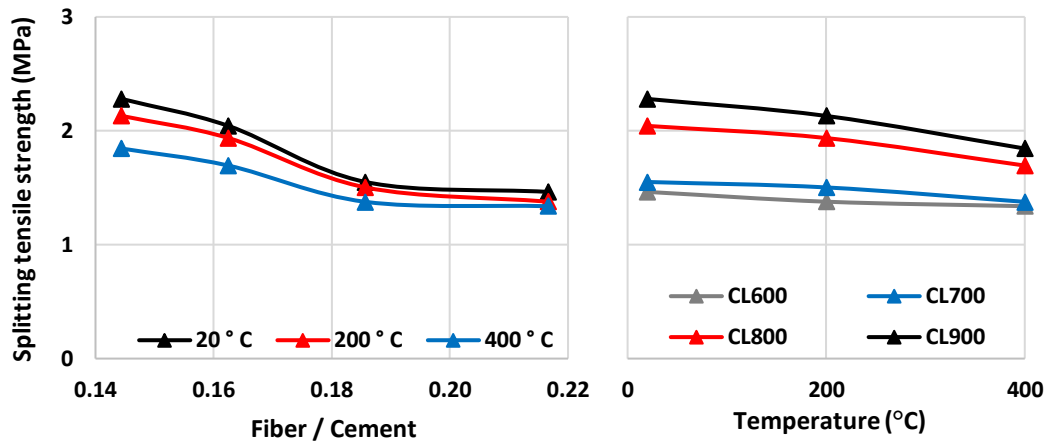


Fig. 5. Variation in the splitting tensile strength of the specimens concerning fiber/cement ratio and temperature after thermal exposure.

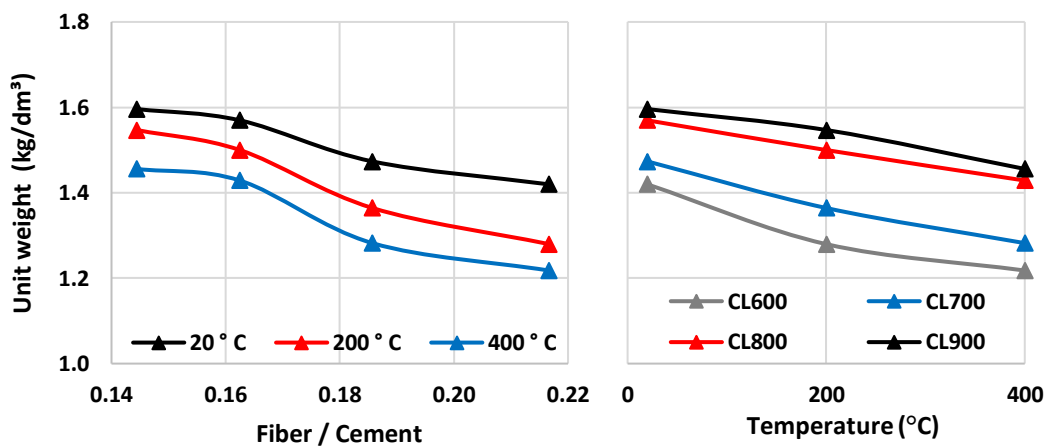


Fig. 6. Changes in the unit weight of specimens depending on the fiber/cement ratio and exposure temperature.

As seen in Fig. 6, unit weight loss was more limited after 200 °C in mixtures with a low fiber/cement ratio and higher cement content. With the increase in temperature to 400 °C, the decrease in unit weight became more pronounced, and the values were measured as 1,218–1,456 kg/dm<sup>3</sup>. Accordingly, total unit weight losses compared with 20 °C reached approximately 14.2% in CL600, 13.0% in CL700, 9.0% in CL800, and 8.8% in CL900. The higher unit weight loss in the CL600 and CL700 samples with a higher fiber-to-cement ratio indicates that the continuity of the internal structure deteriorates more under temperature effects, and porosity increases more markedly. On the other hand, in CL800 and CL900 mixtures, the unit weight loss after temperature exposure is more limited due to the denser cement matrix; however, at 400 °C, it is evident that damage to the internal structure becomes apparent in all mixtures.

### 3.6. Ultrasonic pulse velocity

The ultrasonic pulse velocity (UPV) results after applying temperature are presented in Fig. 7. Cedrus libani clearly shows that the continuity of the internal structure gradually weakens with increasing temperature in cementitious composites reinforced with acicular leaf fiber. UPV values measured at 20 °C were 2.37–2.68 km/h. With the rise in temperature to 200 °C, UPV values de-

creased to 2.23–2.63 km/h; with the increase in temperature to 400 °C, the decrease in UPV became more pronounced, and the values were measured as 2.08–2.49 km/h. The change at 200 °C corresponded to a decrease in the range of approximately 6.2–4.1%, while the change at 400 °C corresponded to a decrease in the range of approximately 12.3–6.9%. For all mixtures, it is seen that the UPV decreases with increasing temperature; this shows that the density of microcracks and discontinuities in the internal structure of the concrete increases with the effect of temperature. The higher UPV losses in the CL600 and CL700 samples with higher fiber-to-cement ratios suggest that the continuity of the internal structure is more sensitive to temperature in these mixtures. In contrast, in the CL800 and CL900 specimens, it was found that the ultrasonic wave transmission paths could be partially conserved due to the denser cement matrix; however, it is understood that internal structural damage becomes evident for all mixtures at the level of 400 °C.

### 3.7. Dynamic modulus of elasticity

The dynamic modulus of elasticity results, as shown in Fig. 8, indicate that the stiffness of cementitious composites reinforced with Cedrus libani acicular leaf fiber decreases significantly with increasing temperature. The

dynamic modulus of elasticity, calculated from unit weight and ultrasonic pulse velocity (UPV), is highly sensitive to the continuity of the concrete's internal structure and microstructural damage. The formula used to calculate the dynamic modulus of elasticity is taken from the ASTM C597 (2020) standard and is shown in Eq. (1). The theoretical expression for the dynamic modulus of elasticity is based on the theory of elastic wave propagation. However, some studies accept a constant value because the Poisson's ratio in cementitious composites cannot always be determined experimentally. In the lit-

erature, the Poisson's ratios of composites made with forest wastes are given as 0.052–0.522 (Ibearugbulem et al. 2019; Güntekin 2022). Similarly, in this study, the Poisson's ratio was assumed to be 0.20, and this assumption was used to calculate the dynamic modulus of elasticity. Additionally, in this study, the dynamic modulus of elasticity was calculated using the unit weight ( $\gamma$ ) parameter instead of density ( $\rho$ ).

$$E_{\text{dynamic}} = V^2 \rho \frac{(1+\nu)(1-2\nu)}{(1-\nu)} \tag{1}$$

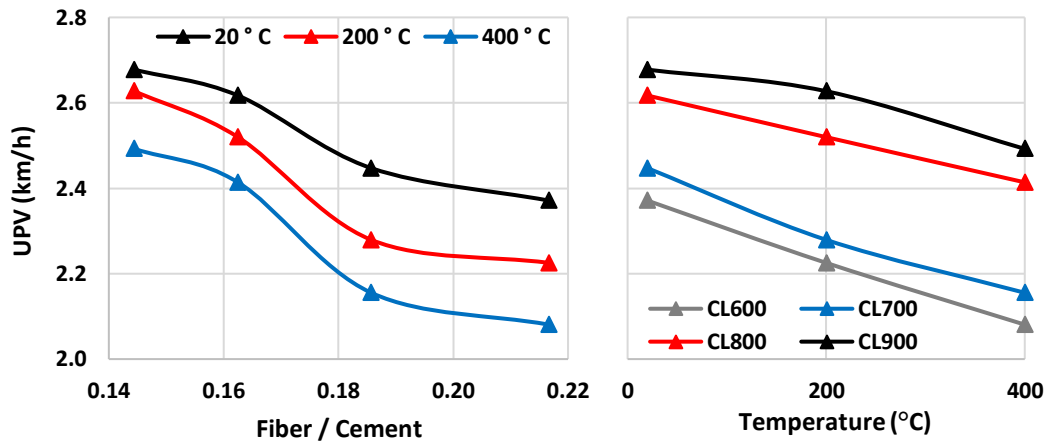


Fig. 7. Effect of fiber/cement ratio and temperature on the UPV of specimens after thermal exposure.

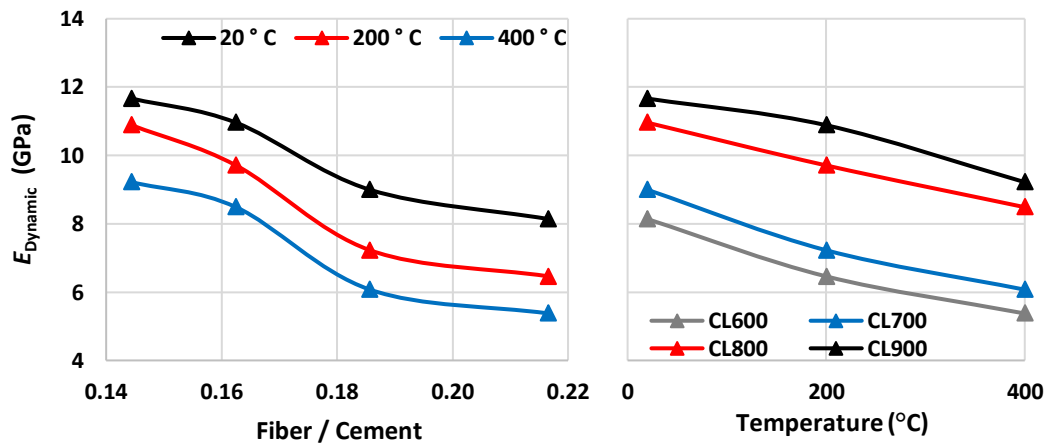


Fig. 8.  $E_{\text{dynamic}}$  of specimens depending on changes in fiber/cement ratio and temperature after thermal exposure.

As the temperature rose to 200 °C, the dynamic modulus of elasticity decreased to 6.2–9.1 GPa, corresponding to a stiffness loss of approximately 7–13% compared with specimens at 20 °C. As shown in Fig. 8, the decrease in the dynamic modulus of elasticity over this temperature range is consistent with the limited decreases observed in unit weight and UPV. As the temperature increased to 400 °C, the decrease in the dynamic modulus of elasticity became more pronounced, reaching 5.5–8.1 GPa. Accordingly, the total stiffness losses compared with the sample at 20 °C ranged from 22–19%. These discontinuities in the internal structure and the increase in microcrack density due to temperature are directly reflected in the dynamic modulus of elasticity through decreases in unit weight and UPV. The greater loss of dynamic modulus of elasticity in CL600 and CL700 mix-

tures with higher fiber/cement ratios suggests that the internal structure is more significantly disrupted after temperature exposure in these mixtures. In contrast, in the CL800 and CL900 specimens, ultrasonic wave transmission paths and unit weight were partially conserved due to the denser cement matrix; however, at 400 °C, rigidity decreased significantly for all mixtures.

#### 4. Conclusions

In this study, the usability of natural fibers derived from dried, fallen acicular leaf of *Cedrus libani* A. Rich. as reinforcement in cementitious composites was extensively evaluated. The fibers underwent a multi-stage extraction and pretreatment process before composite

production; water-soluble components were removed by hot water extraction, the hemicellulosic structure was partially removed, and surface roughness was increased by alkaline treatment. In the mineralization phase with  $\text{Ca}(\text{OH})_2$ , inorganic phase accumulation occurred on the fiber surface. This approach provided controlled surface modification to improve fiber-matrix interfacial interaction. Characterization results showed that the pretreatments induced significant changes in fiber morphology and chemical composition. Increased surface roughness and mineral aggregations were observed in SEM images after processing, and EDS analyses confirmed the transition from a carbon-weighted organic structure to a calcium-rich surface composition. Elemental mapping showed that calcium was inhomogeneous but widely distributed on the fiber surface. These findings support enhanced chemical and mechanical compatibility of the fibers with the cement matrix.

The effect of different fiber/cement ratios on high-temperature behavior was systematically studied in *Cedrus libani* acicular leaf fiber-reinforced cementitious composites produced with aggregate- and additive-free mixtures. Compressive strength results showed that losses were limited (5–9%) up to 200 °C, while at 400 °C, more significant reductions of 8–18% occurred due to microcrack formation and interface weakening. Mixtures with a high fiber/cement ratio were found to reduce strength loss by partially limiting crack progression, especially at 400 °C. Flexural strength results showed a more pronounced response to temperature rise than compressive strength. Strength losses of approximately 10–15% were observed at 200 °C and 13–27% at 400 °C. In mixtures with high cement dosage, proportional losses were higher at 400 °C, whereas in mixtures with a lower fiber/cement ratio, damage development was more controlled thanks to the crack-bridging effect of the fibers. Splitting tensile strength results showed a similar trend; reductions of 3–7% were recorded at 200 °C and 9–19% at 400 °C. In terms of physical properties, unit weight gradually decreased with increasing temperature, and total losses reached 9–14% at 400 °C. UPV results revealed that internal structural continuity weakened with temperature; decreases of 7–12% were observed at 400 °C. This trend is consistent with the increasing density of microcracks and void ratio in the internal structure. Dynamic modulus of elasticity results indicated significant stiffness losses with increasing temperature, consistent with unit weight and ultrasonic transition velocity data. Modulus reductions of approximately 7–13% at 200 °C and 19–22% at 400 °C were calculated. As a result, bio-based cementitious composites produced with *Cedrus libani* A.Rich. acicular leaf fibers largely maintained their mechanical performance at low and medium temperature levels, while fiber-matrix interface damage was decisive at high temperature. These findings show that it is possible to develop sustainable and thermally resistant cementitious composites with appropriate fiber/cement ratio design.

This study has shown that natural fibers from *Cedrus libani* A.Rich. acicular leaf not only offer a sustainable approach to waste assessment but also serve as a technically functional reinforcement material in cementitious composites. Thanks to multi-stage extraction and miner-

alization processes, a chemically and morphologically active structure was created on the fiber surface; this strengthened the fiber-matrix interface interaction and helped maintain mechanical performance, especially at low and medium temperatures. The results showed that when the appropriate fiber/cement ratio is selected, controlled damage development can be achieved in tensile strength under compression, flexural and splitting, and crack propagation is partially limited, while internal structural continuity can be maintained within certain temperature ranges. In addition, unit volume weight, UPV, and dynamic modulus of elasticity data clearly showed that fiber admixture is directly related to microstructural changes under the influence of temperature. This publication scientifically demonstrates that *Cedrus libani* A.Rich. acicular leaf, which are forest waste, constitute a rational alternative in the development of high-added-value, environmentally sustainable cementitious composites that are resistant to thermal effects to a certain extent.

---

#### Acknowledgements

None declared.

#### Funding

The authors received no financial support for the research, authorship, and/or publication of this manuscript.

#### Conflict of Interest

The authors declare no potential conflicts of interest with respect to the research, authorship, and/or publication of this manuscript.

#### Data Availability

The datasets generated and/or analyzed during the current study are not publicly available but are available from the corresponding author upon reasonable request.

#### AI Assistance

No AI-based tools were used in the preparation of this manuscript.

#### Author Contributions

All authors made substantial contributions to the conception and design of the study, acquisition of data, analysis and interpretation of data; drafted or critically revised the manuscript for important intellectual content; and approved the final version to be published.

---

## REFERENCES

- Adamu M, Rehman KU, Ibrahim YE, Shatanawi W (2023). Predicting the strengths of date fiber reinforced concrete subjected to elevated temperature using artificial neural network, and Weibull distribution. *Scientific Reports*, 13, 18649.
- Adamu M, Ibrahim YE, Raut A (2025). High-temperature performance evaluation of sustainable date palm fiber concrete with activated carbon: An MCDM and Weibull analysis approach. *Results in Control and Optimization*, 20, 100602.
- Al-Dala'ien RN, Zaid O, Al-Ezzi MJ, Wani SR (2025). State-of-the-art review on high-temperature performance of plant-based fiber reinforced concrete. *Discover Materials*, 5, 176.
- Alshabrawi HAM, Uysal H (2025). Enhancing the mechanical performance of perforated steel plates through fiber-reinforced composite reinforcement: A finite element analysis study. *Challenge Journal of Structural Mechanics*, 11(4), 174-183.
- Aluko OG, Yatim JM, Kadir MAA, Yahya K (2023). Experimental investigation of residual physical and mechanical properties of kenaf fibre

- reinforced concrete exposed to elevated temperatures. *Fire Technology*, 59, 949-982.
- ASTM C597-16 (2020). Standard test method for pulse velocity through concrete. ASTM International, West Conshohocken, PA, USA.
- Banthia N, Trottier JF (1995). Concrete reinforced with deformed steel fibers, Part I: Bond-slip mechanisms. *ACI Materials Journal*, 92(4), 435-446.
- Baş Fİ (2025). Investigating the effects of glass fiber in enhancing concrete pavement performance. *Challenge Journal of Structural Mechanics*, 11(1), 42-54.
- Bentur A, Mindess S (2007). *Fibre Reinforced Cementitious Composites*. 2nd ed. Taylor & Francis, Abingdon, UK.
- Bilba K, Arsène MA (2008). Silane treatment of bagasse fiber for reinforcement of cementitious composites. *Composites Part A*, 39(9), 1488-1495.
- Canbaz M, Kara İ, Topçu İB (2021). Effect of high temperature on the mechanical behavior of cement-bonded wood composite produced with wood waste. *Challenge Journal of Structural Mechanics*, 7(1), 42-48.
- Cao W, Li J, Marti-Rosselló T, Zhang X (2019). Experimental study on the ignition characteristics of cellulose, hemicellulose, lignin and their mixtures. *Journal of the Energy Institute*, 92(5), 1303-1312.
- Çelik Z, Turan E, Oltulu M, Öner G (2024). Reinforcement of concrete beams using waste carbon-nanoclay-fiberglass laminate pieces. *Challenge Journal of Concrete Research Letters*, 15(1), 1-6.
- Das AK, Agar DA, Rudolfsson M, Kilpeläinen P, Tienaho J, Fernando D (2024). Micromorphology and native extractive behaviour of wood powder. *Scientific Reports*, 14, 25548.
- Dhasindrakrishna K, Pasupathy K, Ramakrishnan S, Sanjayan J (2023). The ambient and elevated temperature performance of hemp fibre reinforced alkali-activated cement foam: Effects of fibre dosage and alkali treatment. *Journal of Building Engineering*, 76, 107131.
- Efe FT (2021). Sedir odununun bazı fiziksel ve mekanik özelliklerinin belirlenmesi üzerine bir araştırma. *Türk Tarım ve Doğa Bilimleri Dergisi*, 8(1), 43-52.
- Feng H, Xia S, Guo A, Huang H, Dai K, Feng Z, Yu Z (2025). Mechanical properties of alkali-activated biomass power plant ash recycled concrete. *Construction and Building Materials*, 481, 141549.
- Fiore V, Scalici T, Valenza A, Di Bella G (2015). A review on basalt fibre and its composites. *Composites Part B*, 74, 74-94.
- Garcez MR, Oliari Garcez E, Machado AO, Gatto DA (2016). Cement-wood composites: Effects of wood species, particle treatments and mix proportion. *International Journal of Composite Materials*, 6(1), 1-8.
- General Directorate of Forestry (2025). Forestry Statistics 2024. <https://www.ogm.gov.tr/tr/e-kutuphane/resmi-istatistikler> [accessed 30-12-2025].
- Grubeša IN, Marković B, Gojević A, Brdarić J (2018). Effect of hemp fibers on fire resistance of concrete. *Construction and Building Materials*, 184, 473-484.
- Güney A, Zimmermann R, Krupp A, Haas K (2016). Needle characteristics of Lebanon cedar (*Cedrus libani* A.Rich.): Degradation of epicuticular waxes and decrease of photosynthetic rates with increasing needle age. *Turkish Journal of Agriculture and Forestry*, 40(3), 386-396.
- Güntekin E (2022). Sedir Odununun (*Cedrus libani* A.) Elastik Sabitleri. *Bartın Orman Fakültesi Dergisi*, 24(3), 436-443.
- Hu M, Lv X, Wang Y, Ma L, Zhang Y, Dai H (2024). Recent advance on lignin-containing nanocelluloses: The key role of lignin. *Carbohydrate Polymers*, 343, 122460.
- Ibearugbulem OM, Amaechi CK, Nwakwasi NL, Anyaogu L, Arimanwa JI, Onyechere IC (2019). Structural characteristics of sawdust-quarry dust composite. *SSRG International Journal of Civil Engineering*, 6(7), 7-12.
- Islam MS, Ahmed SJU (2018). Influence of jute fiber on concrete properties. *Construction and Building Materials*, 189, 768-776.
- Kareem A (2025). A review on date palm fiber as a sustainable reinforcement for concrete applications. *International Journal of Concrete Structures and Materials*, 19(1), 98.
- Li VC (2003). On engineered cementitious composites (ECC). *Journal of Advanced Concrete Technology*, 1(3), 215-230.
- Li K, Deng J, Zhu Y, Zhang W, Zhang T, Tian C, Ma J, Shao Y, Yang Y, Yan-qiu S (2025). Utilization of municipal solid waste incineration fly ash with different pretreatments with gold tailings and coal fly ash for environmentally friendly geopolymers. *Waste Management*, 194, 342-352.
- Long W, Wang Y (2021). Effect of pine needle fibre reinforcement on the mechanical properties of concrete. *Construction and Building Materials*, 278, 122333.
- Lura P, Toropovs N, Justs J, Shakoorioskooie M, Münch B, Griffa M (2025). Mitigation of plastic shrinkage cracking with natural fibers: Kenaf, abaca, coir, jute and sisal. *Cement and Concrete Composites*, 155, 105827.
- Maier D, Manea DL, Tămaş-Gavrea DR, Țiriac A, Costin P (2025). Long-term performance of wood-cement composites: Stabilization versus degradation driven by waste type. *Buildings*, 15(22), 4137.
- Mahzabin MS, Hamid R, Badaruzzaman WHW (2013). Evaluation of chemicals incorporated wood fibre cement matrix properties. *Journal of Engineering Science and Technology*, 8(4), 385-398.
- Melichar T, Dufka A, Dvořák K, Bayer P, Vasas S, Novakova I, Schwarzova I, Bydžovský J (2024). Durability of wood-cement composites with modified composition by limestone and stabilised spruce chips. *Materials*, 17, 6300.
- Merta I, Tschegg EK (2013). Fracture energy of natural fibre reinforced concrete. *Construction and Building Materials*, 40, 991-997.
- Naaman AE (2003). Engineered steel fibers with optimal properties for reinforcement of cement composites. *Journal of Advanced Concrete Technology*, 1(3), 241-252.
- Onuaguluchi O, Banthia N (2016). Plant-based natural fibre reinforced cement composites: A review. *Cement and Concrete Composites*, 68, 96-108.
- Pacheco-Torgal F, Jalali S (2011). Cementitious building materials reinforced with vegetable fibres. *Construction and Building Materials*, 25(2), 575-581.
- Ren G, Gao X, Zhang H (2022). Utilization of hybrid sisal and steel fibers to improve elevated temperature resistance of ultra-high performance concrete. *Cement and Concrete Composites*, 130, 104555.
- Ridha MMS (2024). Combined effect of natural fibre and steel fibre on the thermal-mechanical properties of UHPC subjected to high temperature. *Cement and Concrete Research*, 180, 107510.
- Savastano Jr H, Warden PG, Coutts RS (2003). Potential of alternative fibre cements as building materials for developing areas. *Cement and Concrete Composites*, 25(6), 585-592.
- Silva FA, Chawla N, Toledo Filho RD (2010). Tensile behavior of high performance natural (sisal) fibers. *Composites Science and Technology*, 68(15-16), 3438-3443.
- Şahin HT, Çam E (2022). Properties of gypsum boards made with cedrus tree (*Cedrus libani*) components. Part 2: Chemical and technological properties. *Bartın Orman Fakültesi Dergisi*, 24(2), 202-210.
- Tarhan Y, Tarhan İH, Perrot A (2025). Improving bond performance of 3D-printable earth-based mortar reinforced with jute fibers. *Challenge Journal of Structural Mechanics*, 11(2), 99-105.
- Toledo Filho RD, Ghavami K, England GL, Scrivener K (2005). Development of vegetable fibre-mortar composites of improved durability. *Cement and Concrete Composites*, 27(2), 185-196.
- TS EN 196-1 (2016). Methods of testing cement. Part 1: Determination of strength. Turkish Standards Institution, Ankara, Türkiye.
- Urtekin Y, Çelik Z (2025). Investigation of the effects of re-curing on mechanical properties of basalt-polypropylene hybrid fiber concretes after exposure to high temperature. *Challenge Journal of Structural Mechanics*, 11(1), 14-23.
- Uzun M (2024). Enhancing mechanical properties of foam concrete with sisal fiber reinforcement: An experimental investigation. *Challenge Journal of Concrete Research Letters*, 15(3), 82-89.
- Ünal S, Canbaz M (2025). Photocatalytic activation of fibrous lightweight polymer concrete surfaces under artificial light source. *Challenge Journal of Concrete Research Letters*, 16(1), 15-24.
- Ünal S, Kurt AB, Canbaz M (2025). Impact of wrap quantity on strength of damaged and undamaged CFRP-reinforced structural members. *Challenge Journal of Concrete Research Letters*, 16(3), 133-141.

- Veigas MG, Najimi M, Shafei B (2022). Cementitious composites made with natural fibers: Investigation of uncoated and coated sisal fibers. *Case Studies in Construction Materials*, 16, e00788.
- Yang H, Yan R, Chen H, Lee DH, Zheng C (2007). Characteristics of hemi-cellulose, cellulose and lignin pyrolysis. *Fuel*, 86(12-13), 1781-1788.
- Yousefieh N, Joshaghani A, Hajibandeh E, Shekarchi M (2017). Influence of fibers on drying shrinkage in restrained concrete. *Construction and Building Materials*, 148, 833-845.
- Zhang B, Yin X, Yu H, Zhang Z, Qin W, Hao X (2025). Effects of freezing-microwave assisted alkali treatment on physicochemical and thermomechanical properties of bamboo. *Polymer Testing*, 150, 108905.
- Zhao H, Zhou T, Tang J, Li Z, Yao C, Gao X (2025). Temperature-adaptive mechanism of bamboo fibers for regulating elevated temperature performance of UHPC. *Construction and Building Materials*, 471, 140674.
- Zukowski B, dos Santos ERF, dos Santos Mendonça YG, dos S Silva FDA, Toledo Filho RD (2018). The durability of SHCC with alkali treated curaua fiber exposed to natural weathering. *Cement and Concrete Composites*, 94, 116-125.